Bayesian tip dating reveals heterogeneous morphological clocks in Mesozoic birds

Chi Zhang[1,2,*] and Min Wang[1,2]

September 18, 2018

[1]Key Laboratory of Vertebrate Evolution and Human Origins, Institute of Vertebrate Paleontology and Paleoanthropology, Chinese Academy of Sciences, Beijing 100044, China

[2]Center for Excellence in Life and Paleoenvironment, Chinese Academy of Sciences, Beijing 100044, China

∗Corresponding author: E-mail: zhangchi@ivpp.ac.cn

Running head: BAYESIAN TIP DATING OF MESOZOIC BIRDS

Abstract.—Recently, comprehensive morphological datasets including nearly all the well-recognized Mesozoic birds become available, making it feasible for statistically rigorous methods to unveil finer evolutionary patterns during early avian evolution. However, few quantitative and statistical studies have yet been performed. Here, we exploited the advantage of Bayesian tip dating under relaxed morphological clocks to infer both the divergence times and evolutionary rates while accounting for their uncertainties. We further subdivided the characters into six body regions (i.e., skull, axial skeleton, pectoral girdle and sternum, forelimb, pelvic girdle, and hindlimb) to assess evolutionary rate heterogeneity both along the lineages and across partitions. We observed extremely high rates of morphological character changes during early avian evolution and the clock rates are quite heterogeneous among the six regions. The branch subtending Pygostylia shows extremely high rate in the axial skeleton, while the branches subtending Ornithothoraces and Enantiornithes show very high rates in the pectoral girdle and sternum, and moderately high rates in the forelimb. The extensive modifications in these body regions largely correspond to refinement of the flight capability. The rest of the relatively slow and even rates suggest that there is no dominant selective pressure in favoring of modifications in the skull and pelvis. This study reveals the power and flexibility of Bayesian tip dating implemented in MrBayes to investigate evolutionary dynamics in deep time.

Keywords: Mesozoic birds, tip dating, relaxed clock, MrBayes

Introduction

Birds are one of the most speciose (over 10,000 recognized species) and ecological diverse living vertebrates (Gill 2007). The origin and evolution of birds have long been a hot debate in evolutionary biology, although it has been generally accepted that birds underwent two large-scale radiations during their 160 million years evolution, one for the stem groups in the Cretaceous, and the other for the crown groups in the Paleogene (Mayr 2009; Prum et al. 2015; Wang and Zhou 2017). Over the last few years, numerous well-preserved Mesozoic bird fossils have been described (Chiappe and Meng 2016; Wang and Zhou 2017), and consensus has been approached regarding their systematic relationships (O'Connor and Zhou 2013; Wang et al. 2017; 2018). These wealthy data have significantly bridged the large morphological gap between birds and their non-avian theropod predecessors (O'Connor and Zhou 2015; Wang and Zhou 2017), and demonstrated their evolutionary success related to novel traits. Expanded morphological characters that cover the major Mesozoic avian groups with chronological data become accessibly recently (Wang and Lloyd 2016), making it possible to trace the early avian evolution more quantitively and to address important questions such as the divergence times of the major clades and the patterns of morphological character changes in and between lineages (Brusatte et al. 2014; Lloyd 2016). However, few quantitative and statistical studies for early avian evolution have yet been performed.

In a previous study, Wang and Lloyd (2016) investigated evolutionary rate heterogeneity in Mesozoic birds under maximum parsimony using a large morphological dataset containing 262 characters and 58 taxa (Wang et al. 2015). The approach was stepwise: first to infer the most parsimonious trees, then to inform the internal node ages using certain *ad hoc* measures, and last to obtain the branch rates from dividing the number of parsimonious changes by the time durations along the corresponding branches. It did not account for the uncertainties of tree topology, times and rates statistically, and was unable to model the evolutionary process explicitly. The dataset was then extended to 280 characters and 68 taxa recently (Wang and Zhou 2018), with newly recognized species and significantly revised morphological character scorings. Moreover, we revised this dataset according to (Field et al. 2018), mainly focusing on the cranial morphology of Ichthyornithiformes and Hesperornithiformes. The modified dataset contains nearly all the well-recognized Mesozoic birds and represents the most comprehensive morphological characters at present, thus provides more power to unveil finer evolutionary patterns and becomes applicable to more statistically rigorous methods.

We further subdivided the characters into six partitions, each representing a different anatomical region (i.e., skull, axial skeleton, pectoral girdle and sternum, forelimb, pelvic girdle, and hindlimb), to assess evolutionary rate heterogeneity. Partitioned analysis has been attempted by Clarke and Middleton (2008) on a much smaller dataset of stem birds under a Bayesian non-clock model to examine the

77 branch-length variations across three body regions. Since each branch length was a
78 product of geological time duration and evolutionary rate, the two elements could not
79 be distinguished without a time tree and clock assumption.

80 Here, we exploited the advantage of tip dating to infer both the divergence times
81 and evolutionary rates while accounting for their uncertainties in a coherent Bayesian
82 statistical framework. The technique was originally developed for analyses combining
83 both morphological and molecular data (Pyron 2011; Ronquist et al. 2012a; 2016;
84 Zhang et al. 2016; Lee 2016; Gavryushkina et al. 2016) and has been termed as
85 "total-evidence dating". It has also been productively applied to morphological data
86 only (Lee et al. 2014; Bapst et al. 2016; Matzke and Wright 2016; King et al. 2017)
87 and we use "tip dating" for that matter. This approach has the essential strengths of
88 incorporating various sources of information from the fossil record directly in the
89 analysis, modeling the speciation process explicitly through a probabilistic model
90 allowing for parameter inference and model selection, and utilizing the state-of-the-art
91 developments in Bayesian computation.

92 Materials and methods

93 *Morphological data*

94 The morphological data used in this study is based on Wang and Zhou (2018)
95 which is extended and revised from Wang et al. (2015). Character scorings for
96 *Ichthyornis dispar*, *Hesperornis regalis*, *Parahesperornis alexi*, and *Baptornis*

97 *advenus* were further revised according to Field et al. (2018). The modified dataset
98 consists of 280 morphological characters and 68 operational taxonomic units
99 (Dromaeosauridae as the outgroup, 65 Mesozoic and 2 extant birds). Detailed
100 character descriptions are listed in Supplementary Material.
101 The characters were further partitioned into six anatomical regions to assess
102 evolutionary rate heterogeneity across these regions: skull (53 characters), axial
103 skeleton (36 characters), pectoral girdle and sternum (48 characters), forelimb (65
104 characters), pelvic girdle (23 characters), and hindlimb (55 characters). Each partition
105 included more than 20 characters to ensure sufficient information for inference.

106 *Tip dating*

107 In Bayesian tip dating framework, we infer the posterior probability distribution of
108 the model parameters, which combines the information from the morphological
109 characters (likelihood) and the priors (including the distributions of the fossil ages and
110 the other parameters in the tree model and clock model). For the likelihood, the Mkv
111 model (Lewis 2001) was used for the character state substitution with gamma rate
112 variation across characters. The gamma distribution has mean 1.0 ($\alpha = \beta$) and was
113 approximated with four discrete categories (Yang 1994). 36 characters were defined
114 as ordered (Supplementary Information), which means instantaneous change is only
115 allowed between adjacent states, the rest of the characters were thus unordered. The

prior for gamma shape α was exponential(1), while the priors for the time tree and the relaxed clock model parameters are described in detail in the following sections.

In order to root the tree properly and infer the evolutionary rates more reliably, we applied five topology constraints as Aves, Pygostylia, Ornithothoraces, Enantiornithes and Ornithuromorpha (Fig. 1), each of which forms a monophyletic clade.

The posterior distribution was estimated using Markov chain Monte Carlo (MCMC). We executed two independent runs with four chains (one cold and three hot) per run for 40 million iterations and sampled every 2000 iterations. The first 25% samples were discarded as burn-in for each run, and the remaining samples from the two runs were combined after checking consistency between runs.

Tree model

The fossilized birth-death process (Stadler 2010; Heath et al. 2014; Gavryushkina et al. 2014; Zhang et al. 2016) was used to model speciation, extinction, fossilization and sampling, which gave rise to the prior distribution of the time tree $\mathcal{T}$. The process starts at the root with two lineages sharing the same origin. Each lineage bifurcates with a constant rate λ and goes extinct with a constant rate μ. Concurrently, each lineage is sampled with a constant rate ψ and is removed from the process upon sampling with probability r. Extant taxa are sampled with probability ρ. The explicit derivation of the probability density function was given in Gavryushkina et al. (2014, Equation 4). When the removal probability $0 \leq r < 1$, the sampled tree may contain

136 fossil ancestors (i.e., fossils with sampled descendants), while setting $r = 1$ disables
137 fossil ancestors (i.e., all fossils are at the tips).

138 The age of each fossil bird was assigned a uniform prior with lower and upper
139 bounds from the corresponding stratigraphic range (Supplementary Information). The
140 root age was assigned an offset exponential prior with mean 169 Ma (slightly older
141 than the first appearance datum of Dromaeosauridae) and minimum 153 Ma (slightly
142 older than the first appearance datum of *Archaeopteryx*). For inference, we
143 reparametrized the speciation, extinction and sampling rates and assigned priors as d
144 $= \lambda - \mu - r\psi \sim$ exponential(100) with mean 0.01, $v = (\mu + r\psi)/\lambda$ and $s = \psi/(\mu + \psi) \sim$
145 uniform(0, 1). The sampling proportion of extant taxa (*Anas* and *Gallus*) was set to
146 0.0002, based on the number of described living bird species around ten thousands
147 (Gill and Wright 2006).

148 *Clock model*

149 We applied the independent gamma (white noise) relaxed clock model (Lepage et
150 al. 2007) to investigate evolutionary rate heterogeneity both along the tree and across
151 the six anatomical regions (partitions). The model was reparametrized aiming to
152 articulate the relative rates. Specifically, the model assumes that the substitution rate
153 (clock rate, in unit of substitutions per character per myr) of branch i in partition j, c_{ij},
154 is a product of the mean rate c and the relative rate r_{ij} (i.e., $c_{ij} = cr_{ij}$), and r_{ij} is gamma
155 distributed with mean 1.0 and variance $\sigma_j/(t_i c)$, where t_i is the geological time duration

of branch i (i = 1, …, $2m$ – 2, j = 1, …, n). Thus, the clock model has n + 1 parameters (c, σ_1, …, σ_n), and there are $(2m - 2) \times n$ independent rates in the tree. The relative rate r_{ij} serves as a multiplier to the mean rate. Large deviation of r_{ij} from 1.0 indicates severe heterogeneity of the morphological clock, while r_{ij}'s all being similar to 1.0 models a somewhat strict clock. The branch length (distance, in unit of substitutions per character) in the Mkv likelihood calculation, b_{ij}, is the product of time duration t_i and clock rate c_{ij} (i.e., $b_{ij} = t_i c_{ij} = t_i c r_{ij}$).

The prior used for the mean clock rate c was gamma(2, 200) with mean 0.01 and standard deviation 0.007, and that for σ_j was exponential(10).

Results and Discussion

There is no clear evidence for us to believe that all fossils are at the tips *a priori*, however, we encountered severe mixing problem in the MCMC when allowing fossil ancestors while partitioning the morphological characters into six anatomical regions. When treating the characters as a single partition on the other hand, we were able to achieve good mixing both allowing and disallowing fossil ancestors (setting r = 0 and r = 1 respectively). Thus, we first show the results without partitioning the data and compare the difference between with and without fossil ancestors, then we focus on the evolutionary rate heterogeneity when the data is partitioned (only under r = 1). In general, the parameter estimates are quite similar whether fossil ancestors are allowed, the difference is more dramatic whether the data is partitioned (see below).

176 *Single partition*

177 The phylogeny estimated from tip dating allowing fossil ancestors (r = 0) is shown
178 in Figure 1. The tree is well resolved, with a few polytomies mainly nested within
179 Enantiornithes that represent the uncertainty of the taxa relationships. This topology
180 agrees with previously published trees in the placements of the major clades (Wang et
181 al. 2015; Wang and Lloyd 2016; Wang and Zhou 2018). The root age is estimated at
182 162.56 (153.00, 171.26) Ma (see also Table 1), which covers the fixed age of 168.7
183 Ma (1 myr older than the first appearance datum of Dromaeosauridae using the
184 minimum branch length method) (Wang and Lloyd 2016). The posterior age of
185 Dromaeosauridae is 154.90 (141.66, 167.69) Ma, mainly within Late Jurassic, while
186 the prior range expands the whole Cretaceous (66.0, 167.7). As the posterior mean
187 relative rate at the branch of Dromaeosauridae is 1.08 (close to 1.0), the similarity of
188 the morphological characters informs a short time span. The mean ages of the
189 divergences of Pygostylia, Ornithothoraces and Enantiornithes are about 6–8 myr
190 older than the fixed ages in the previous study (Wang and Lloyd 2016). We
191 emphasize that the age estimates using tip dating integrates all available sources of
192 information but the minimum branch length method only used the first appearance
193 datum of the oldest taxa thus might underestimate the ages.

194 When disallowing fossil ancestors (r = 1), one concern might arise is that some
195 node ages might be overestimated due to forcing every tip to be the result of
196 speciation. However, the difference from allowing fossil ancestors (r = 0) is really

197 minor in our case. The node ages are only about 1–2 myr older if not otherwise
198 similar (Fig. 1). The topologies in these two cases are almost identical, except for two
199 places—one is the placement of *Cruralispennia* which becomes unresolved in the big
200 polytomy within Enantiornithes, the other is *Archaeornithura* which becomes a
201 sibling of *Tianyuornis*. In fact, the estimated proportion of fossil ancestors is 0.13
202 (0.06, 0.21), indicating most fossils are indeed tip fossils. *Enaliornis* and
203 *Archaeornithura* have the highest posterior probabilities of being ancestral (0.95 and
204 0.93 respectively).

205 The evolutionary rates are thus very similar for the two cases and we only show the
206 result under $r = 0$ (Fig. 1). The mean clock rate (c) is estimated around 0.01
207 substitutions per character per myr (i.e., approximately one character-state change per
208 100 million years) (Table 1). The relative clock rate at each branch represents the
209 deviation from the mean rate. We observe extremely high rates during early avian
210 evolution (Fig. 1). The relative rates at the two branches from Aves to Pygostylia are
211 6.63 (0.97, 17.49) and 5.34 (0.01, 15.52), and accelerate to 10.89 (0.00, 32.5) at the
212 branch subtending Ornithothoraces. High rates are also encountered along the early
213 branches of Ornithuromorpha, then slow down substantially towards crownward
214 branches including the one leading to extant birds. Enantiornithes shows even higher
215 rate of 11.24 (1.49, 30.75) when it diverges from Ornithuromorpha in the Early
216 Cretaceous, and the rates decrease dramatically in its later history. These observations
217 concurs with previous comparative studies that birds underwent a large scale of

diversification in tandem with the dinosaur-bird transition (Benson and Choiniere 2013; Lee et al. 2014; Wang and Lloyd 2016).

Six partitions

The evolutionary rates inferred above are averaged across all morphological characters. Further partitioning the data into six anatomical regions make it feasible for us to estimate refined evolutionary rates both along branches and across partitions. Different partitions have their own independent rate variations while sharing the same tree topology and geological time duration (i.e., single time tree $\mathcal{T}$). As mentioned above, the mixing was very poor if fossil ancestors were allowed ($r = 0$) and independent runs did not give consistent estimates. The difficulty was probably due to limited data in each partition interfered with inefficient reversible-jump MCMC (rjMCMC) algorithm (Green 1995) implemented. Further investigations are required. At the moment, we just show the result disallowing fossil ancestors ($r = 1$) which simplifies the tree structure with no need for rjMCMC. In this case, the major clades inferred in the tree are unchanged, although a few taxa with large uncertainties shuffle a bit (Supplementary Figs S1–S6). Comparing with the node ages estimated under a single partition, those at the early avian diversifications are slightly older (Fig. 1, see also Table 1) while the younger ages become more similar. The age differences are more dramatic whether the data is partitioned than whether fossil ancestors are allowed.

The rates of morphological character changes are quite heterogeneous among the six regions during early avian evolution (Fig. 2), although the mean rate (*c*) estimated is almost identical as before (Table 1). The branch subtending Pygostylia shows extremely high rate in the axial skeleton (Fig. 2, Supplementary Fig. S2), which is one order of magnitude higher than in the rest five regions. Clearly, the high rate observed here indicates extensive morphological changes in the vertebral column, and the most recognizable change is that a long tail consisting of over 20 caudal vertebrae in *Archaeopteryx* and *Jeholornis* is replaced by a short element called pygostyle which is formed by the fusion of several caudal most vertebrae (Wang and Zhou 2017). The transition from long to short tail is functionally important for the evolution of powered flight in birds: a short tail could forward the gravitational center, and with attached feathers become indispensable for the avian flight apparatus (Gatesy and Dial 1996). The branches subtending Ornithothoraces and Enantiornithes show very rapid morphological changes in the pectoral girdle and sternum, and moderately high rates in the forelimb (Fig. 2, Supplementary Figs S3&S4). In comparison, the corresponding rates in the other regions are close to 1.0 with slight variation. These results suggest that most of the changes related to the shoulder and forelimb are close to the origin of Ornithothoraces, for example, the presence of an ossified sternum with a keel (attachment for the major flight muscle in modern birds) and further elongate forelimb (O'Connor and Zhou 2015), contributing to the refinement of flight capability. The rapid morphological changes towards Enantiornithes correspond to

their unique shoulder morphology relative to the ancestor Ornithothoraces; for instance, enantiornithines have a sternum with a caudally restricted keel and an elongate acromion of the scapula, both of which are the major components of the flight apparatus in birds (Chiappe and Walker 2002; Wang and Zhou 2017). Previous morphometric study suggested that Enantiornithes have different flight style compared with other Mesozoic birds in terms of limb proportion (Dyke and Nudds 2009). The rest of the relatively slow and even rates suggest that there is no dominant selective pressure in favoring of modifications in the skull and pelvis.

When we compared the evolutionary rates between Enantiornithes and Ornithuromorpha across the six regions by summarizing the mean relative rates within each clade (excluding *Anas*, *Gallus* and their common ancestral branch), the differences are not striking, with medians uniformly close to 1.0 (Fig. 3). However, significantly high rates (outliers) are detected along some early diverging branches within these two clades, and a slowdown in more crownward branches (Fig. 3, Supplementary Figs S1–S6), suggesting that morphological changes are rapid in early diversifications and the process slows down subsequently due to saturated ecological niches for these two avian groups, as proposed in previous study (Wang and Lloyd 2016).

To test the robustness of age estimates to the root age prior and the impact on evolutionary rates in consequence, we halved and doubled the range between the mean and minimal in the original prior, that is, using offset-exp(153, 161) and

offset-exp(153, 185) priors for the root age. This comparison showed slightly varied posterior age estimates deep in the tree. For the root age in particular, the estimates are 170.83 (161.33, 179.78) and 174.31 (164.34, 184.77) under the smaller and larger prior mean respectively. Thus, the conclusion of evolutionary rate heterogeneity above is not changed as the age differences are minor comparing with the significantly high rates which are usually one order of magnitude higher than 1.0.

Another concern related to the accuracy of age estimates might be the nonuniform fossil record both in its geographical and stratigraphic distribution. Although more complicated models allowing fossil sampling rate vary over time are available (Gavryushkina et al. 2014; Zhang et al. 2016), it is not practical to apply in our case to make reliable inference. The current model assuming constant sampling rate is a balance between model complexity (number of parameters) and model adequacy (accommodating rate variation across lineages). Since the focus of our study is on the deep divergence times and the evolutionary rates, the rich fossil record in Early Cretaceous provided a great deal of information to produce reliable estimates deep in the tree. For the age estimates in the Late Cretaceous or later, biases might be severe due to limited fossil record. In particular, the divergence time of Anas and Gallus has been estimated at the early Eocene (Prum et al. 2015) associated with high evolutionary rates at the crown. In comparison, we inferred much younger age of 9.46 (4.57, 15.07) Ma with a long, low-rate ancestral branch. The underestimation was

mainly due to lacking fossil or node calibrations within that clade, so the posterior estimate tended to be similar to the prior.

The gamma shape parameter (α) of character rate variation is larger than 1.0 (Table 1), indicating that the evolutionary rates are fairly homogeneous across characters. Note this gamma distribution models rate variation across characters and is independent of the gamma distributions for rate variation across branches in the relaxed clock model.

Partitioning the data is a common practice in molecular phylogenetic analyses (Nylander et al. 2004; Brown and Lemmon 2007). The different partitions may correspond to different genes and may also correspond to different codon positions in a protein-coding gene. On the other hand, morphological characters are typically treated as a single partition unless sufficient characters are available (Lee 2016) or simple model assumptions are made (Clarke and Middleton 2008). While successfully demonstrating the different evolutionary dynamics modeled by independent rate parameters in the six partitions, we note that the variance is very large (Fig. 2, widths of the error bars) due to limited number of characters in each partition. Further effort of coding more characters would refine the resolution.

In summary, the Bayesian tip dating approach implemented in MrBayes is a powerful and flexible tool to simultaneously estimate the tree topology, divergence times, evolutionary rates, and the other parameters of interest while accounting for their uncertainties. In the priors, we are able to incorporate the uncertainty of each

fossil age, model the speciation, extinction, fossilization and sampling process explicitly, and take advantage of the relaxed clock model to investigate rate variation cross branches and partitions. It is feasible to integrate all available sources of information in the analysis, rather than discarding certain information or uncertainties in the parsimony and stepwise approach. Although the focal species are Mesozoic birds in this study, tip dating is a general framework applicable to a wide range of taxonomic groups with potential future extensions to the theoretical model and practical implementation.

Availability

The models described above were implemented in MrBayes version 3.2.7 (Ronquist et al. 2012b. https://github.com/NBISweden/MrBayes; last accessed September 10, 2018).

Supplementary Material

Data available from the Dryad Digital Repository: http://dx.doi.org/-.

Funding

This research is supported by the 100 Young Talents Program of Chinese Academy of Sciences (to C.Z.). M.W. is supported by National Natural Science Foundation of China (41722202).

Acknowledgments

We sincerely thank three anonymous reviewers for constructive criticisms of the original article and excellent suggestions for improvement.

References

Bapst D.W., Wright A.M., Matzke N.J., Lloyd G.T. 2016. Topology, divergence dates, and macroevolutionary inferences vary between different tip-dating approaches applied to fossil theropods (Dinosauria). Biol. Lett. 12:20160237.

Benson R.B.J., Choiniere J.N. 2013. Rates of dinosaur limb evolution provide evidence for exceptional radiation in Mesozoic birds. Proc. Biol. Sci. 280:20131780–20131780.

Brown J.M., Lemmon A.R. 2007. The importance of data partitioning and the utility of Bayes factors in Bayesian phylogenetics. Syst. Biol. 56:643–655.

Brusatte S.L., Lloyd G.T., Wang S.C., Norell M.A. 2014. Gradual assembly of avian body plan culminated in rapid rates of evolution across the dinosaur-bird transition. Curr. Biol. 24:2386–2392.

Chiappe L.M., Meng Q. 2016. Birds of stone: Chinese avian fossils from the age of dinosaurs. Johns Hopkins University Press.

Chiappe L.M., Walker C.A. 2002. Skeletal morphology and systematics of the

357 Cretaceous Euenantiornithes (Ornithothoraces: Enantiornithes). In: Chiappe L.M.,
358 Witmer L.M. editors. Mesozoic birds: above the heads of dinosaurs. California:
359 University of California Press. pp. 240–267.

360 Clarke J.A., Middleton K.M. 2008. Mosaicism, modules, and the evolution of birds:
361 Results from a Bayesian approach to the study of morphological evolution using
362 discrete character data. Syst. Biol. 57:185–201.

363 Dyke G.J., Nudds R.L. 2009. The fossil record and limb disparity of enantiornithines,
364 the dominant flying birds of the Cretaceous. Lethaia. 42:248–254.

365 Field D.J., Hanson M., Burnham D., Wilson L.E., Super K., Ehret D., Ebersole J.A.,
366 Bhullar B.-A.S. 2018. Complete Ichthyornis skull illuminates mosaic assembly of
367 the avian head. Nature. 557:96–100.

368 Gatesy S.M., Dial K.P. 1996. Locomotor modules and the evolution of avian flight.
369 Evolution. 50:331–340.

370 Gavryushkina A., Heath T.A., Ksepka D.T., Stadler T., Welch D., Drummond A.J.
371 2016. Bayesian total-evidence dating reveals the recent crown radiation of
372 penguins. Syst. Biol. 66:57–73.

373 Gavryushkina A., Welch D., Stadler T., Drummond A.J. 2014. Bayesian inference of
374 sampled ancestor trees for epidemiology and fossil calibration. PLoS Comput.
375 Biol. 10:e1003919.

376 Gill F.B. 2007. Ornithology. New York: W.H. Freeman.

377 Gill F.B., Wright M.T. 2006. Birds of the world: recommended English names.
378 Princeton: Princeton University Press.

379 Green P.J. 1995. Reversible jump Markov chain Monte Carlo computation and
380 Bayesian model determination. Biometrika. 82:711–732.

381 Heath T.A., Huelsenbeck J.P., Stadler T. 2014. The fossilized birth-death process for
382 coherent calibration of divergence-time estimates. Proc. Natl. Acad. Sci. USA.
383 111:E2957–66.

384 King B., Qiao T., Lee M.S.Y., Zhu M., Long J.A. 2017. Bayesian morphological
385 clock methods resurrect placoderm monophyly and reveal rapid early evolution in
386 jawed vertebrates. Syst. Biol. 66:499–516.

387 Lee M.S.Y. 2016. Multiple morphological clocks and total-evidence tip-dating in
388 mammals. Biol. Lett. 12:20160033.

389 Lee M.S.Y., Cau A., Naish D., Dyke G.J. 2014. Morphological clocks in paleontology,
390 and a mid-Cretaceous origin of crown Aves. Syst. Biol. 63:442–449.

391 Lepage T., Bryant D., Philippe H., Lartillot N. 2007. A general comparison of relaxed
392 molecular clock models. Mol. Biol. Evol. 24:2669–2680.

393 Lewis P.O. 2001. A likelihood approach to estimating phylogeny from discrete

394 morphological character data. Syst. Biol. 50:913–925.

395 Lloyd G.T. 2016. Estimating morphological diversity and tempo with discrete
396 character-taxon matrices: implementation, challenges, progress, and future
397 directions. Biological Journal of the Linnean Society. 118:131–151.

398 Matzke N.J., Wright A. 2016. Inferring node dates from tip dates in fossil Canidae:
399 the importance of tree priors. Biol. Lett. 12:20160328.

400 Mayr G. 2009. Paleogene fossil birds. Berlin Heidelberg: Springer-Verlag.

401 Nylander J.A.A., Ronquist F., Huelsenbeck J.P., Nieves-Aldrey J.L. 2004. Bayesian
402 phylogenetic analysis of combined data. Syst. Biol. 53:47–67.

403 O'Connor J.K., Zhou Z. 2013. A redescription of *Chaoyangia beishanensis* (Aves)
404 and a comprehensive phylogeny of Mesozoic birds. Journal of Systematic
405 Palaeontology. 11:889–906.

406 O'Connor J., Zhou Z. 2015. Early evolution of the biological bird: perspectives from
407 new fossil discoveries in China. Journal of Ornithology. 156:333–342.

408 Prum R.O., Berv J.S., Dornburg A., Field D.J., Townsend J.P., Lemmon E.M.,
409 Lemmon A.R. 2015. A comprehensive phylogeny of birds (Aves) using targeted
410 next-generation DNA sequencing. Nature. 526:569–573.

411 Pyron R.A. 2011. Divergence time estimation using fossils as terminal taxa and the

origins of Lissamphibia. Syst. Biol. 60:466–481.

Ronquist F., Klopfstein S., Vilhelmsen L., Schulmeister S., Murray D.L., Rasnitsyn A.P. 2012a. A total-evidence approach to dating with fossils, applied to the early radiation of the Hymenoptera. Syst. Biol. 61:973–999.

Ronquist F., Lartillot N., Phillips M.J. 2016. Closing the gap between rocks and clocks using total-evidence dating. Philos. Trans. R. Soc. Lond. B Biol. Sci. 371: 20150136.

Ronquist F., Teslenko M., van der Mark P., Ayres D.L., Darling A., Höhna S., Larget B., Liu L., Suchard M.A., Huelsenbeck J.P. 2012b. MrBayes 3.2: efficient Bayesian phylogenetic inference and model choice across a large model space. Syst. Biol. 61:539–542.

Stadler T. 2010. Sampling-through-time in birth-death trees. J. Theor. Biol. 267:396–404.

Wang M., Lloyd G.T. 2016. Rates of morphological evolution are heterogeneous in Early Cretaceous birds. Proc. Biol. Sci. 283:20160214.

Wang M., O'Connor J.K., Pan Y., Zhou Z. 2017. A bizarre Early Cretaceous enantiornithine bird with unique crural feathers and an ornithuromorph plough-shaped pygostyle. Nat Commun. 8:14141.

Wang M., O'Connor J.K., Zhou Z. 2018. A taxonomical revision of the

431 Confuciusornithiformes (Aves: Pygostylia). Vertebrata Palasiatica.

432 Wang M., Zheng X., O'Connor J.K., Lloyd G.T., Wang X., Wang Y., Zhang X., Zhou
433 Z. 2015. The oldest record of ornithuromorpha from the early cretaceous of China.
434 Nat Commun. 6:6987.

435 Wang M., Zhou Z. 2017. The evolution of birds with implications from new fossil
436 evidences. In: Maina N.J., editor. The Biology of the Avian Respiratory System.
437 Cham: Springer International Publishing. pp. 1–26.

438 Wang M., Zhou Z. 2018. A new confuciusornithid (Aves: Pygostylia) from the Early
439 Cretaceous increases the morphological disparity of the Confuciusornithidae.
440 Zoological Journal of the Linnean Society. in press.

441 Yang Z. 1994. Maximum likelihood phylogenetic estimation from DNA sequences
442 with variable rates over sites: approximate methods. J. Mol. Evol. 39:306–314.

443 Zhang C., Stadler T., Klopfstein S., Heath T.A., Ronquist F. 2016. Total-evidence
444 dating under the fossilized birth-death process. Syst. Biol. 65:228–249.

445

446 Table 1. Posterior distributions (mean and 95% HPD interval) of model parameters

	single partition, $r = 0$	single partition, $r = 1$	six partitions, $r = 1$
α	1.81 (1.35, 2.31)	1.82 (1.35, 2.31)	1.80 (1.33, 2.27)
$d = \lambda - \mu - r\psi$	0.010 (0.00087, 0.022)	0.010 (0.00075, 0.021)	0.010 (0.00042, 0.020)
$v = (\mu + r\psi)/\lambda$	0.98 (0.94, 1.00)	0.93 (0.81, 1.00)	0.92 (0.79, 1.00)
$s = \psi/(\mu + \psi)$	0.028 (0.00047, 0.075)	0.33 (0.00051, 0.90)	0.35 (0.00059, 0.90)
t_{mrca}	162.56 (153.00, 171.26)	164.17 (153.33, 173.34)	172.61 (164.01, 180.81)
c	0.012 (0.0090, 0.015)	0.011 (0.0083, 0.014)	0.010 (0.0081, 0.012)
σ or σ_1	0.058 (0.035, 0.084)	0.058 (0.036, 0.084)	0.070 (0.026, 0.12)
σ_2			0.069 (0.028, 0.12)
σ_3			0.057 (0.028, 0.090)
σ_4			0.053 (0.025, 0.087)
σ_5			0.042 (0.0017, 0.084)
σ_6			0.061 (0.029, 0.095)

447

448

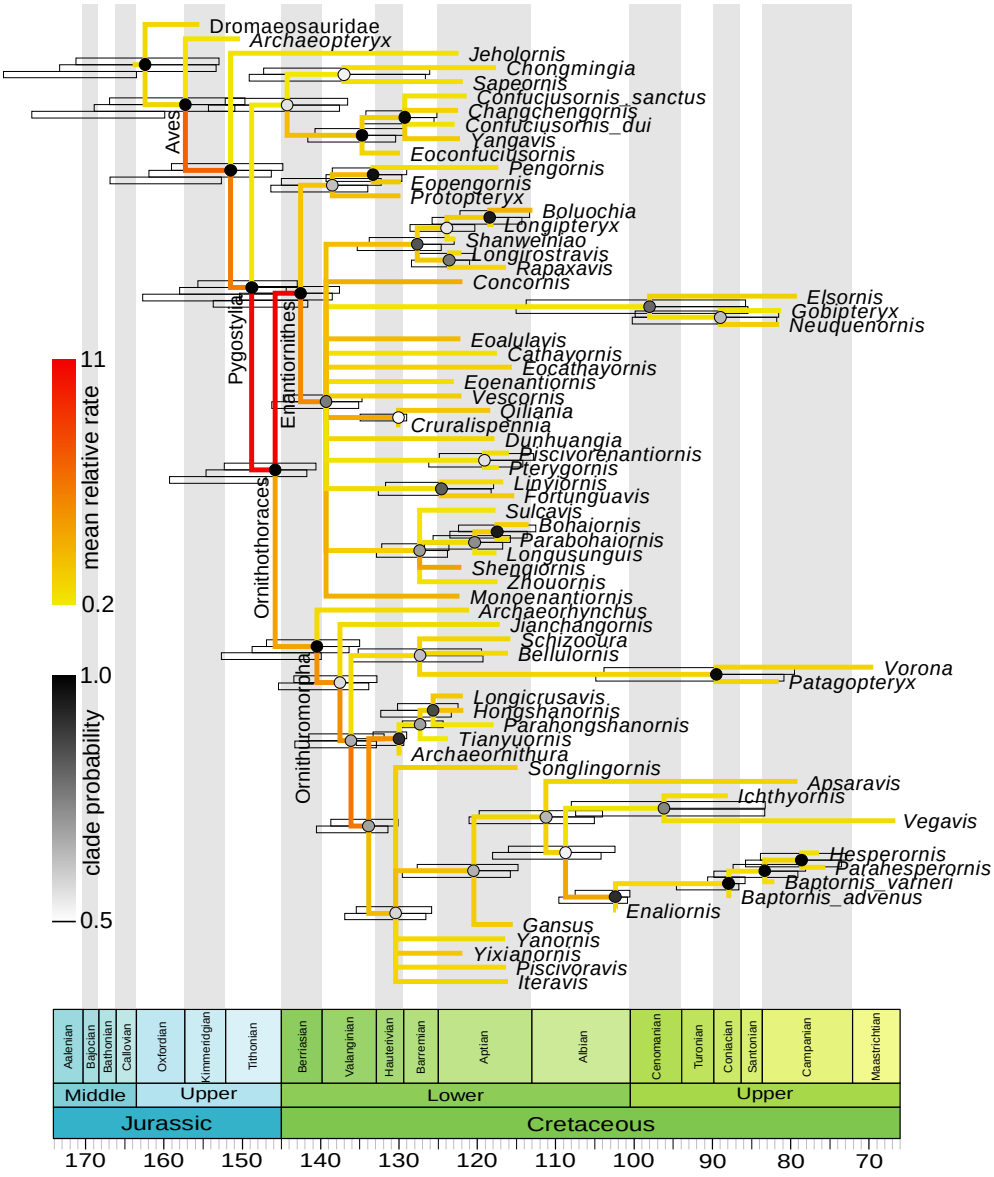

Figure 1. Dated phylogeny (time tree) of Mesozoic birds. The topology (majority-rule consensus tree) shown is inferred allowing fossil ancestors (r = 0) without partitioning the morphological characters. The node ages in the tree are the posterior medians and the shade of each circle represents the posterior probability of the corresponding clade. The color of the branch represents the mean relative clock rate at that branch. The error bars on the top (in blue) at the internal nodes denote the 95% HPD intervals of

457 age estimates. In comparison, the error bars below (if present, in cyan) denote the 95%
458 HPD intervals when disallowing fossil ancestors (r = 1) under a single partition.
459 Additionally, the error bars shown at the early avian diversifications (in green) are the
460 95% HPD intervals of age estimates when the characters are partitioned into six
461 anatomical regions and disallowing fossil ancestors (r = 1). The two extant species
462 (*Anas* and *Gallus*) were included in the analyses but not shown in the representation
463 (as a sister clade of *Vegavis*).

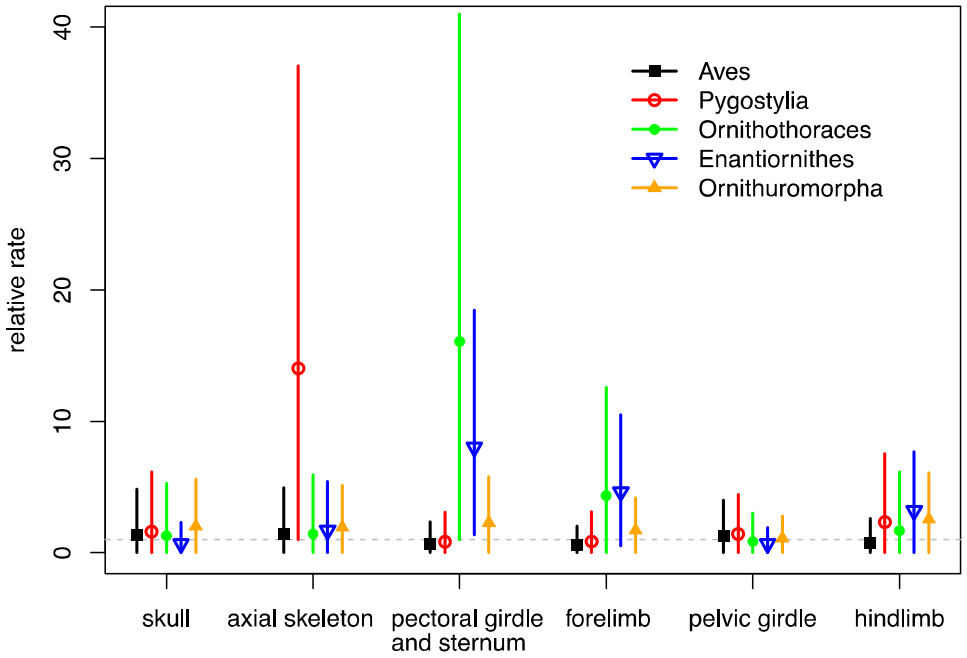

464

465

466 Figure 2. Posterior estimates of the relative clock rates along the branches subtending

467 the major transitions of early avian evolution for six anatomical regions of the bird

468 body. The dot and error bar denote the mean and 95% HPD interval for each estimate.

469 The horizontal dashed line indicates the mean relative rate of 1.0 in the relaxed model.

470

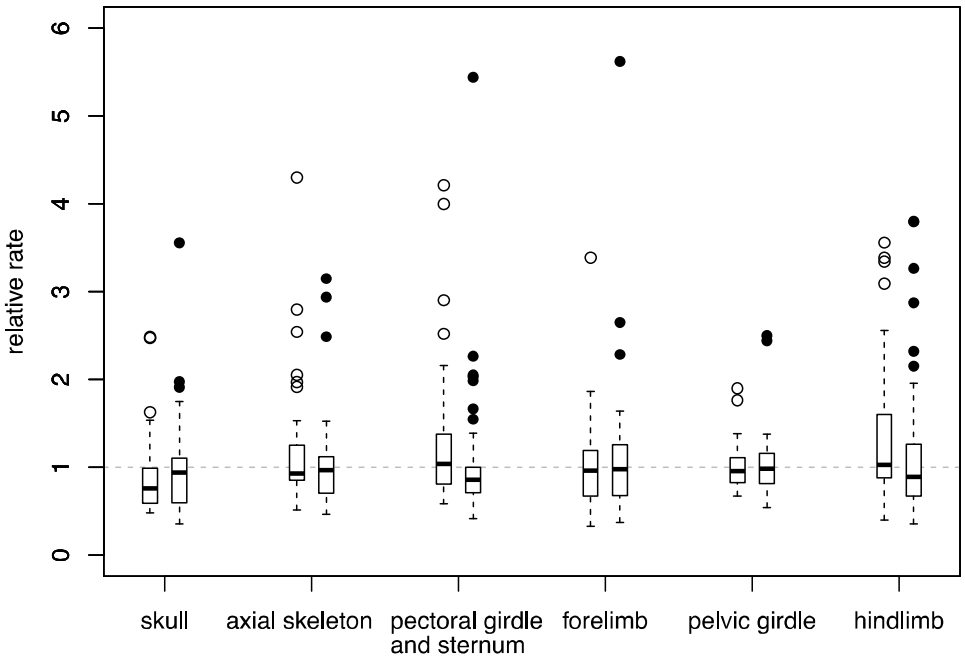

Figure 3. Boxplots summarizing the mean relative clock rates across branches in the Enantiornithes clade (left) and Ornithuromorpha clade (right) respectively, for the six anatomical regions. The box denotes the 1st, 2nd (median) and 3rd quartiles while the dots are the outliers. The horizontal dashed line indicates the mean relative rate of 1.0 in the relaxed clock model.